JOURNAL OF SOLID STATE CHEMISTRY 115, 283–290 (1995)

$WTh_8Zr_{18}F_4O_{53}$: A New Superstructure of Fluorite Type, Associating Anion-Excess and Anion-Deficient Blocks

J. P. Laval[1] and A. Taoudi

Laboratoire de Matériaux Céramiques et Traitements de Surface, U.R.A. C.N.R.S. n° 320, 123 Avenue A. Thomas, 87060 Limoges Cedex, France

Received January 31, 1994; in revised form August 17, 1994; accepted August 19, 1994

The crystal structure of a new complex oxyfluoride $WTh_8Zr_{18}F_4O_{53}$, a member of a wide series $MTh_8Zr_{18}(F, O)_{57}$, was solved on the basis of single-crystal data obtained on a four-circle diffractometer CAD-4 (R = 4.2%). The space group is $Fm\bar{3}m$(Z = 4) and the lattice derives from fluorite-type one by the relationship a = 1578.5 pm = 3 a_F. This structure is characterized by a fcc cationic array with full cationic ordering and by an ordered distribution of two kinds of structural units: (i) anion-excess fluorite units containing "cuboctahedral" clusters, similar to those observed in anion-excess fluorite phases, e.g., β-U_4O_9 and KY_3F_{10} (these units are composed of six ZrO_8 square antiprisms, sharing edges with eight $ThFO_9$ polyhedra, about a cuboctahedral anionic cavity occupied by an extra F anion); (ii) Anion-deficient fluorite units, based on the association, about a single WFO_5 octahedron, of six ZrO_7 and six ZrO_8 polyhedra, in a similar way as in "stabilized" zirconia and Ln_nO_{2n-2} rare earth oxides (e.g., Pr_7O_{12}). Then, $WTh_8Zr_{18}F_4O_{53}$ is the first example of a fluorite superstructure composed of an ordered intergrowth of anion-excess $Th_8Zr_6F_3O_{30}$ and anion-deficient $WZr_{12}FO_{23}$ fluorite blocks. $WTh_8Zr_{18}F_4O_{53}$ is the anion-excess fluorite superstructure the poorest in anions ever characterized: $MX_{2.11}$. The possibility, demonstrated for the first time, to associate in a fluorite structure anion-excess and anion-deficient parts constitutes a conceptual advance in the knowledge of nonstoichiometry.

INTRODUCTION

The nonstoichiometry in fluorite type, either by introduction of anion excess or by creation of anionic vacancies, is the subject of many studies. There is now a general agreement about the presence in these phases of "clusters" associating dopant and host cations, anionic vacancies, and/or interstitial anions.

In the anion-deficient domain MX_{2-x}, ordered superstructures show the presence of extended clusters about anionic vacancies, associating MX_6 octahedra, MX_7 polyhedra, and MX_8 cubes. These clusters are long-range ordered in rather complex ways but, until now, only some of these structures have been completely solved (1–5) because of systematic twinning of crystals and incomplete long-range ordering of the phases.

In the anion-excess composition range MX_{2+x}, two kinds of clusters were isolated in ordered superstructures:

— "cuboctahedral" clusters, associating six MX_8 square antiprisms about a cuboctahedral anionic cavity accommodating the anion excess (e.g., β-U_4O_9, KY_3F_{10}, $Ca_{13+\delta}$ (Y, $Ln)_{6-\delta}F_{44-\delta}$(tveitit), ... (6–8))

— "column" clusters, associating MX_8 isolated square antiprisms in double linear columns (e.g., Pb_3ZrF_{10}, K_2NbF_7 (9)).

All these kinds of well defined clusters are used as models to understand the defect structure in the homologous anion-deficient and anion-excess solid solutions. Their direct insertion, in variable proportions and in a more or less modified form, into fluorite structure, without high distortion, allows us to explain the structural features of many solid solutions.

The present work describes the crystal structure of a new ordered variety of fluorite phase, $WTh_8Zr_{18}F_4O_{53}$, associating such clusters in a very original way.

PREPARATION AND CHARACTERIZATION OF $WTh_8Zr_{18}F_4O_{53}$

During a systematic study of mixed thorium–zirconium oxyfluorides heated at 1000–1100°C in Ni sealed tubes, we observed, for compositions very close to the ZrO_2–ThO_2 binary system, the formation of single crystals of green color. As a contamination by Ni of the sealed tubes was suspected, an EDAX analysis was performed on a single crystal but did not reveal the presence of nickel (<1%). However, on a suggestion of D. J. M. Bevan, the presence of chromium, acting as an impurity in Ni (even nominally pure!), was detected in a small quantity, and direct synthesis by addition of CrF_3 to the previous mixtures allowed us to obtain in almost pure

[1] To whom correspondence should be addressed.

0022-4596/95 $6.00

form this new phase (with small proportions of unreacted thoria and zirconia) for the composition $CrTh_8Zr_{18}F_7O_{50}$. Its X-ray powder pattern revealed a cubic symmetry with a strong subcell of fluorite type (space group: $Fm\bar{3}m$) and a superlattice of the same space group with the a parameter $a = 3\ a_F = 1575.9$ pm. Owing to the complex formula and the interest in solving the structure of this new kind of fluorite superstructure, we tried to prepare good single crystals, but systematically, inclusions of powder were present inside crystals. Then, various attempts to prepare isotypic phases were performed and beautiful single crystals of orange color were obtained by substitution of CrF_3 by WO_3 in a mixture containing a slight excess of fluorine (starting composition WO_3, $18ZrO_2$, $6.5ThO_2$, $1.5ThF_4$). The synthesis conditions were: heating for 2 days at 1200°C in Ni sealed tubes (without Cr impurities!), slow decreasing of the temperature from 1200 to 900°C, 2-day annealing at this last temperature, and then water quenching.

STRUCTURE DETERMINATION

A single crystal of radius $R = 0.05$ mm and of octahedral shape was selected and recorded on a four-circle diffractometer CAD-4; 3358 reflections were measured under the conditions reported in Table 1. After averaging equivalent reflections, 327 independent reflections corresponding to $I > 4\sigma(I)$ were used to determine cationic sites by the direct method (SHELXTL (10)). Owing to the high absorption of the single crystal ($\mu = 38$ mm^{-1}, $\mu R \approx 2$), corrections were applied to the data, using a psi-scan method. All cationic positions were located and refined. Then, five anionic sites were detected after Fourier-difference calculations, and refined. However, important anomalies on the O(3) site ($B > 30.10^4$ pm^2 in $32f$ site x, x, x; $x = 0.08$) were significant of a high delocalization of anions about this site, clearly evident on Fourier-difference maps. After several attempts, the best solution was obtained by a delocalization on a more general $96k$ site x, z, z, with $x = 0.049$ and $z = 0.080$. The occupancy of this site was also refined to $\tau = 0.24(4)$; however, in spite of its splitting, the thermal vibration of this anion was rather high ($B \approx 4.10^4$ pm^2) and some residues of electron density persisted about the refined position. Attempts to refine together two statistically occupied close sites failed.

After refinement of the five anions with isotropic thermal vibration coefficients and of the cations with anisotropic ones, the R factor stabilized to 4.3%, but a very diffuse electron density peak appeared on Fourier-difference maps about the $4b$ position 1/2, 1/2, 1/2. Refinement of a thermal vibration coefficient on this fixed F(6) site failed, but it was possible to refine either a split 24e site x, 1/2, 1/2 (with $x \approx 0.53$) or a $32f$ site x, x, x ($x \approx 0.53$) but with very high thermal vibration factors ($B > 6.10^4$ pm^2) and standard deviations. Such a result could be considered as unsignificant although a refinement of the occupancy revealed a value in agreement with a fully occupied $4b$ site. However, this dilute site corresponds to a well known anionic position presenting similar characteristics in various anion-excess fluorites (11), and it was kept in a central $4b$ site with a fixed B value for a final refinement to $R = 4.2\%$. A last Fourier-difference map

TABLE 1
Data Collection and Refinement Parameters

Symmetry	Cubic
Space group	$Fm\bar{3}m$
Cell parameter	$a = 1578.5(6)$ pm
Absorption coefficient	$\mu = 38$ mm^{-1} ($\mu R = 2$)
Absorption	Psi-scan
Radiation	Mo$K\alpha$
Recording range	$0 \le h \le +12$; $0 \le k \le +22$; $0 \le l \le +22$
Number of observed reflections	3358
Number of independant reflections	344 ($R_{av} = 0.054$)
Number of weak reflections	22
Number of reflections with $I/\sigma(I) > 4$	327
Number of refined variables	25
	No weighting scheme
	No extinction correction.
	$R = 0.042$; $R_w = 0.042$

TABLE 2
Atomic Parameters and Isotropic (B) and Anisotropic ($U_{ij} \times 10^4$) Temperature Factors for $WTh_8Zr_{18}F_4O_{53}$

	Site	Coordinates x	y	z	B or B_{eq} ($\times 10^{-4}$) pm^2	τ
W	4*a*	0	0	0	0.46(2)	1
Zr(1)	24*e*	0.3156(2)	0	0	1.01(4)	1
Zr(2)	48*h*	0.32850(9)	0.32850	0	1.36(3)	1
Th	32*f*	0.34544(3)	0.34544	0.34544	1.05(1)	1
F(1)	8*c*	1/4	1/4	1/4	0.9(5)	1
O(2)	48*i*	1/2	0.1241(6)	0.1241	1.0(2)	1
O(3)	96*k*	0.049(4)	0.080(3)	0.080	4.(2)	0.24(4)
O(4)	48*g*	0.0794(8)	1/4	1/4	1.1(2)	1
O(5)	96*k*	0.0826(4)	0.0826	0.2283(6)	1.0(1)	1
F(6)	4*b*	1/2	1/2	1/2	6[a]	1.

Atom	U_{11}	U_{22}	U_{33}	U_{23}	U_{13}	U_{12}
W	209(7)	209	209	0	0	0
Zr(1)	124(11)	129(7)	129	0	0	0
Zr(2)	176(6)	176	161(9)	0	0	54(7)
Th	132(3)	132	132	8(2)	8	8

[a] Fixed value.

TABLE 3
Main Interatomic Distances in $WTh_8Zr_{18}F_4O_{53}$

Bond	Distance (pm)	Bond	Distance (pm)	Bond	Distance (pm)
W–Zr(2)	382.9(2)	W–O(3)	195.(6)	F(1)–O(4)	269.(1)
Zr(1)–Zr(1)	411.7(4)	Zr(1)–O(2)	217.8(4)	O(2)–O(2)	277.(1)
Zr(1)–Zr(2)	353.6(2)	Zr(1)–O(5)	230.1(9)	O(2)–O(5)	275.(1)
Zr(1)–Th	348.2(1)	Zr(1)–F(6)	250.(50)	O(3)–O(3)	253.(9)
Zr(2)–Zr(2)	353.6(2)	Zr(2)–O(4)	215.4(8)		263.(6)
Zr(2)–Th	368.3(1)	Zr(2)–O(3)	218.(6)		209.(7)
Th–Th	487.9(1)		273.(5)	O(3)–O(5)	240.(5)
	426.1(2)	Zr(2)–O(5)	211.5(4)		284.(6)
Th–F(1)	260.9(1)	O(4)–O(4)	251.(3)		
Th–O(2)	253.3(4)	O(4)–O(5)	266.5(7)		
Th–O(4)	243.9(7)	O(5)–O(5)	261.(1)		
Th–O(5)	244.9(9)	F(6)–O(2)	250.(30)		

did not reveal any significant peak except some residues, mainly about the Zr(2) and O(3) sites, reflecting a partly statistical character of the structure to be discussed further. The introduction of a weighting scheme did not improve this result.

The structural parameters are gathered in Table 2 and the main interatomic distances in Table 3. Although the results of the refinement could not predict a possible O/F order on anionic sites, anions are labeled in these tables according to the results of the bond valence calculations.

STRUCTURE DESCRIPTION

I. Anionic Polyhedra

— *Zr(1) cation* (Fig. 1) is located in a ZrO_8 square antiprism including four Zr–O(2) bonds of 217.8 pm and four opposite much longer Zr–O(5) bonds of 230.1 pm. A ninth Zr–F(6) bond corresponds to the very diffuse F(6) anionic site. Such an 8 + 1 coordination can be sometimes observed for Zr, e.g., in $Na_7Zr_6F_{31}$ (11) in which a weakly linked F anion, homologous to F(6), is present.

— *Th cation* is in 10-fold coordination in a hybrid $ThFO_9$ polyhedron, which can be considered as a cube with one corner replaced by an O(2)–O(2)–O(2) triangular face (Fig. 2). This kind of polyhedron, half cube, half icosahedron, is called a "centaur" polyhedron by Bevan. Th–O fairly regular bonds (244–253 pm) are completed by one longer Th–F(1) bond (260.9 pm).

— *W cation*, localized in a 4*a* site (0, 0, 0), is only coordinated to O(3) anions in a 96*k* site x, z, z; $x = 0.049$, $z = 0.080$, statistically occupied in a proportion closely corresponding to 6 O(3) anions for each W cation. The anions of this 96*k* site are split from a 32*f* site x, x, x; $x = 0.08$ which would correspond, if it was fully occupied, to a cubic coordination for W^{6+} unsuitable for this cation. Then, the W cation is very likely coordinated to a more or less distorted anionic octahedron (Fig. 3b). Four different orientations of this octahedron are possible, as shown in Fig. 3a, and their statistical superposition agrees with the $Fm\bar{3}m$ symmetry. The W–O(3) distance of 195 pm corresponds to the usual W–O bonds (≈190 pm), in spite of the difficulty in exactly localizing O(3) anions in this statistical arrangement.

— *Zr(2) cations*, directly connected to a WO_6 octahedron, are not equivalent in the local structures resulting from each of the four orientations of this octahedron. Two different kinds of anionic polyhedra, only differing by the number and the relative position of O(3) anions, are possible:

(*i*) a ZrO_8 polyhedron (Fig. 4a), intermediate between a bicapped trigonal prism and a distorted cube and comprising six rather regular Zr–O bonds (four Zr–O(5) at 211.5 pm, two Zr–O(4) at 215.4 pm) and two much longer Zr–O(3) at 273 pm.

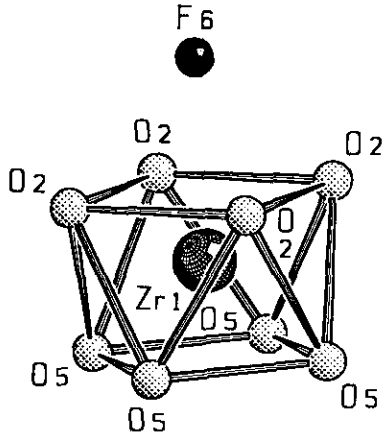

FIG. 1. $Zr(1)O_8$ square antiprism, with an O(2)–O(2)–O(2)–O(2) square face capped by an extra, weakly bonded F(6) anion.

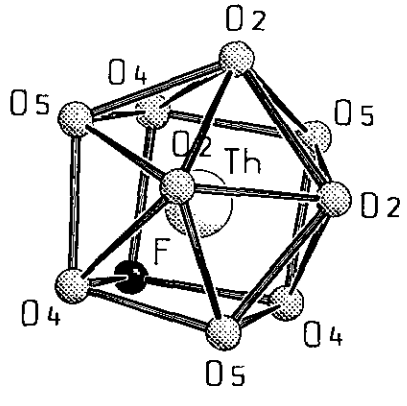

FIG. 2. $ThFO_9$ "centaur" polyhedron.

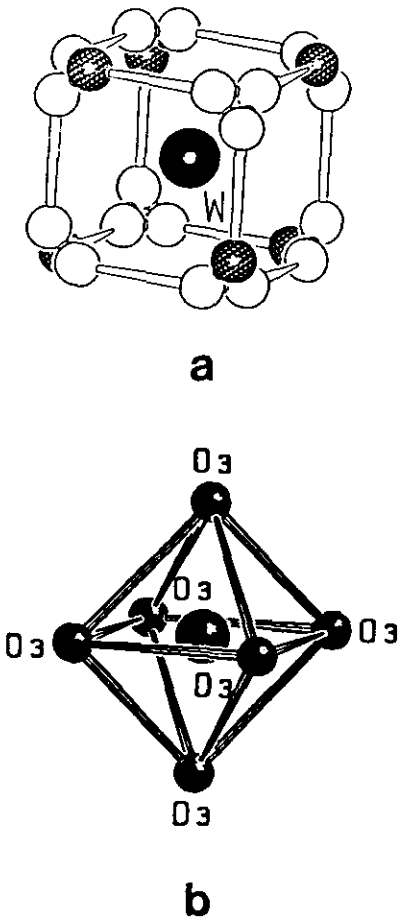

FIG. 3. (a) W atom statistically surrounded by 24 anions. Six anions, represented as small dark spheres, correspond to an octahedron represented in (b). Four different orientations of this octahedron are possible.

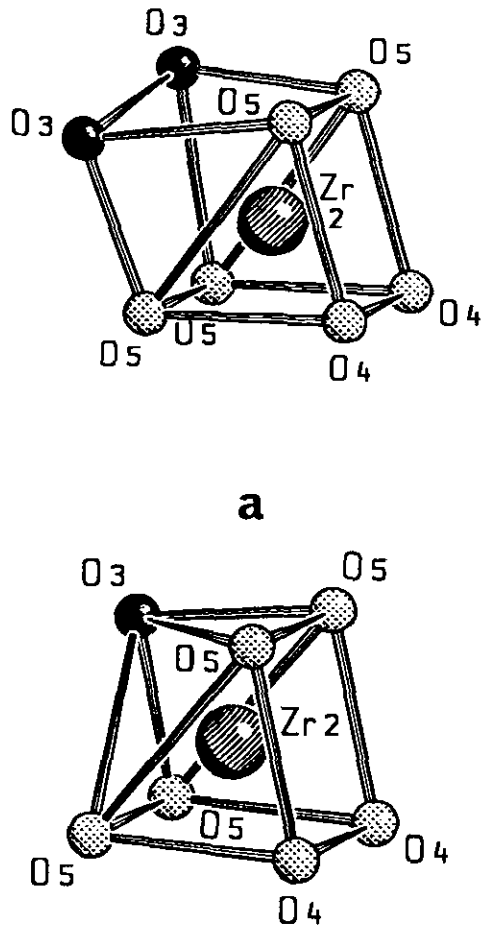

FIG. 4. (a) $Zr(2)O_{6+2}$ polyhedron and (b) $Zr(2)O_7$ polyhedron. These polyhedra differ only by the number and the respective positions of O(3) anions of the WO_6 octahedron to which they are connected.

(ii) a ZrO_7 monocapped trigonal prism (Fig. 4b) with regular Zr–O bonds. The trigonal prism is the same as in ZrO_8, but the seventh Zr–O(3) distance is much closer (218 pm).

For a given orientation of a WO_6 octahedron, both configurations have the same number of polyhedra.

II. O/F Order in Anionic Sites

Many oxyfluorides, especially for cations of high coordination (>6), present a perfect O/F ordering, e.g., $PbZr_3F_6O_4$ (12), $PbZr_6F_{22}O_2$ (13), and $BaTh_6F_{24}O$ (14). As the scattering factors are very close for O^{2-} and F^- anions, the best way to identify both anions is the bond valence method. We used this method, in the way developed by Brown (15) to calculate the bond valence of the seven anion sites. In spite of approximations resulting from the statistical character of some atomic positions, this calculation, reported in Table 4, clearly shows that the F(1) site, coordinated to four Th^{4+} cations at a rather long distance (Th–F(1) = 260.9 pm), is a fluoride anion (v = 0.93). In the same way, O(4) and O(5) are undoubt-

TABLE 4
Electrostatic Bond Valences in $WTh_8Zr_{18}F_4O_{53}$

Site	Coordination	Bond valence	
		Exp.	Theor.
F(1)	4Th	0.93	1
O(2)	2Zr + 2Th	1.77	2
O(3)	3Zr + 1W	1.67	2
O(4)	2Zr + 2Th	2.06	2
O(5)	3Zr + 1Th	2.06	2
F(6)	1 – 6 Zr	0.2	1

edly oxide anions (v = 2.06). The F(6) site corresponds, as in $Na_7Zr_6F_{31}$, to loosely bonded (v = 0.2) F anions trapped in a cuboctahedral cavity.

For the O(2) and O(3) sites, a slight charge deficit for O^{2-} anions (v = 1.77 and 1.67 respectively) could result from the statistical presence of some F anions: the O(2) anions are the inner corners of a cuboctahedral cluster, as discussed later. The [2 + 2] coordination of this site is well suited to F anions, but O/F disorder in this symmetrical environment was never observed and seems unlike.

Conversely, O/F disorder in structures containing octahedra, e.g., in ReO_3-type structures like $TiOF_2$, TaO_2F . . . , is very frequent. Moreover, the MO_6 octahedra can be occupied by M cations of various charge in the $MTh_6Zr_{18}(F, O)_{57}$ series (from +3 for Cr to +6 for W). All these observations strongly suggest that the O(3) site accepts in a disordered way the remaining F anions in variable proportion (their number is indeed greater when the M charge is lower), in order to ensure a local compensation of charges about the M cation.

Then the most convenient anionic distribution in the W^{6+} phase is $WTh_8Zr_{18}F(1)_2O(2)_{12}O(3)_5F(3)O(4)_{12}O(5)_{24}F(6)$, with the presence of a WFO_5 octahedron.

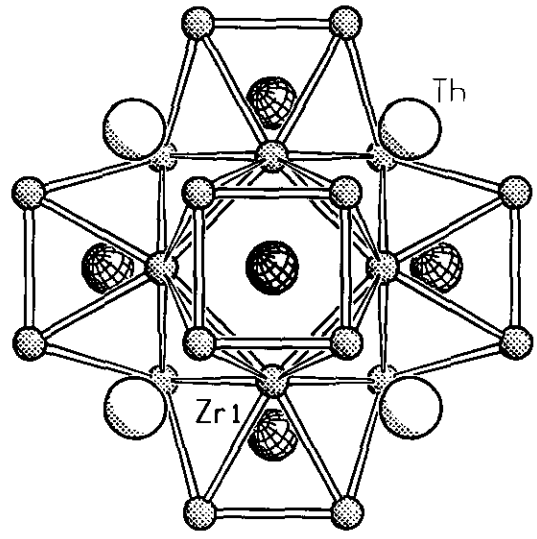

FIG. 5. Projection, onto the xy plane, of a Zr_6FO_{36} cuboctahedral cluster, surrounded by eight $ThFO_9$ "centaur" polyhedra. It is built from six $Zr(1)O_8$ corner-shared square antiprisms enclosing an O_{12} cuboctahedral cavity occupied by an extra F(6) anion.

III. Association of the Polyhedra in Clusters

The structure of $WTh_8Zr_{18}F_4O_{53}$ is composed of the association of five different kinds of polyhedra, representing four different coordinations: 6, 7, 8, and 10. Two sorts of anionic clusters, well known in structures deriving from fluorite type, can be evidenced:

— *a cuboctahedral cluster* (Fig. 5), built from six ZrO_8 square antiprisms sharing corners about a $O(2)_{12}$ cuboctahedron. The inside of this cluster is occupied, as for $Na_7Zr_6F_{31}$ (11), $PbZr_6F_{22}O_2$ (13), and the M_nF_{2n+5} series of anion-excess fluorites (16), by an extra F(6) anion. In all these quoted phases, this extra anion is not exactly in the center of the cuboctahedral cavity but shifted along a three fold axis of the cuboctahedron from ≈ 50 to 70 pm. A similar statistical shift of F(6) anion from the (1/2, 1/2, 1/2) center of the cuboctahedral $O(2)_{12}$ cavity of $WTh_8Zr_{18}F_4O_{53}$ explains the difficulty in localizing this weakly bonded anion and its very high thermal vibration factor.

The cuboctahedral cluster is completed by eight $ThFO_9$ "centaur" polyhedra, connected to the square antiprisms by O(2)–O(2)–O(2) triangular faces. The composition of the complete structural unit is then $Th_8Zr_6F_3O_{30}$. This formula corresponds for an independent anion-excess fluorite-type superstructure to a member of the series M_nX_{2n+5}, with n = 14, accommodating five excess anions for each cluster. Indeed, cuboctahedral clusters are created in an fluorite structure by a cooperative rotation of the six square faces of an empty O_8 cube, transforming this cube in a O_{12} cuboctahedron. This local structural operation creates four new anionic sites (five if the inner of the cuboctahedron is filled by an extra 13th anion), giving the possibility to introduce excess anions in a fluorite structure without highly modifying its volume. Therefore, such clusters can be integrated in high proportion in fluorite without macroscopic distortion. In fact, in this structural process, edge-shared cubes are replaced by corner-shared square antiprisms, which causes a lenghtening of intercationic distances. Conversely, "centaur" polyhedra are connected to square antiprisms by triangular faces, which induces a contraction of the corresponding cation–cation distances. In the present cluster, this double influence is effective, as the Zr(1)–Zr(1) distance is 411.7 pm and Th–Zr(1) only 348.2 pm.

$WTh_8Zr_{18}F_4O_{53}$ is the first fluorite phase, with β-U_4O_9 (6), to contain almost exclusively O anions inside the cuboctahedral cluster. The excess of O^{2-} anions implies charge compensation by highly charged cations not only in the square antiprisms but also in the "centaur" polyhedra. Only cations of great size and charge as Th^{4+} and U^{4+} can play this compensating role, which partly explains the scarcity of oxides with an anion-excess fluorite structure.

— *an anion-deficient cluster* (Fig. 6a), very similar to those existing in fluorite phases containing ordered anionic vacancies, as, e.g., Pr_7O_{12} (1), UY_6O_{12} (2), Tl_6TeO_{12} (17), or $Zr_{10}Sc_4O_{26}$ (3). It is composed of a central WFO_5 octahedron surrounded by six $Zr(2)O_7$ polyhedra, along a

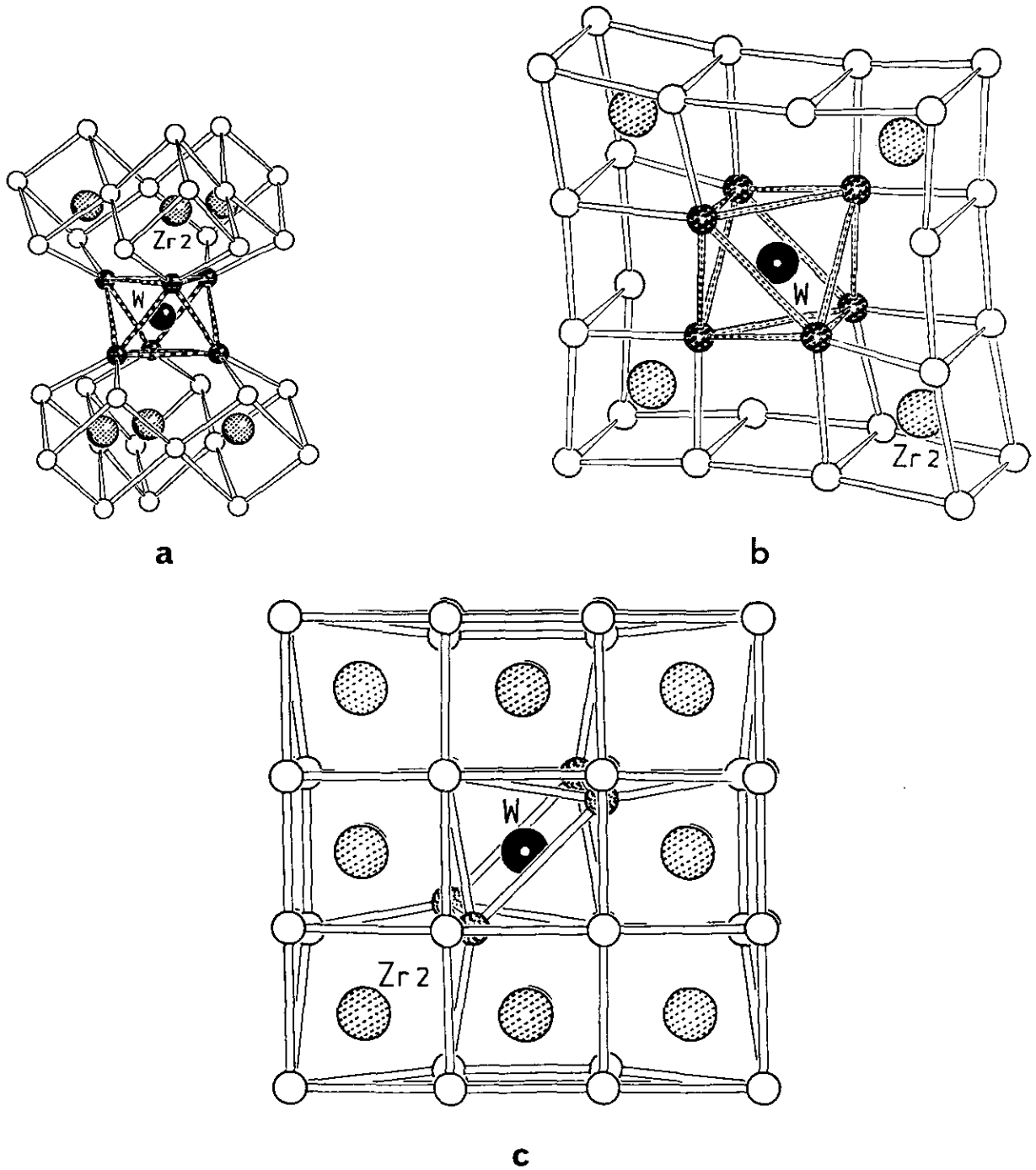

FIG. 6. (a) Anion-deficient cluster, associating one WFO_5 octahedron and six $Zr(2)O_7$ polyhedra, seen along a three-fold axis of the fluorite subcell. (b) Perspective view of one sheet of polyhedra, emphasizing the connections of a WFO_5 octahedron with the adjacent Zr(2) polyhedra. The relationship to the fluorite structure, via the creation of two anionic vacancies, is obvious. (c) Projection onto the *xy* plane of a $WZr_{12}FO_{23}$ anion-deficient structural unit, associating six $Zr(2)O_7$ and six $Zr(2)O_8$ polyhedra about a WFO_5 octahedron. Only one of the four possible orientations of the octahedron is represented.

three-fold axis of the fluorite lattice. The perspective view of the Fig. 6b shows the connection of this octahedron with four adjacent $Zr(2)O_7$ and $Zr(2)O_8$ polyhedra and emphasizes its integration in a fluorite structure, via the creation of two anionic vacancies. The association of the anion-deficient cluster with its six adjacent $Zr(2)O_8$ polyhedra (considered as fluorite distorted cubes) forms an almost cubic structural unit of formula $WZr_{12}FO_{23}$,

shown in Fig. 6c. The Figure 7 shows the homologous unit described in UY_6O_{12} (2), a rhombohedral ($n = 7$) member of the M_nX_{2n-2} series of anion-deficient fluorite phases. The comparison of both units (Figs. 6c and 7) shows that they derive from similar 13-cation fluorite blocks by creation of two anionic vacancies, transforming an MX_8 cube in an octahedron and the adjacent cubes in MX_7 or MX_8 polyhedra. In the $n = 7$ member of the M_nX_{2n-2} series, each octahedron is connected to 12 MX_7 polyhedra, compared to 6 ZrO_7 and ZrO_8 polyhedra for the $WZr_{12}FO_{23}$ unit. That is a consequence of the greater closeness of the UO_6 octahedra one to another, correlated to the higher number of anionic vacancies in $UY_6O_{12}(MO_{1.714})$. If $WZr_{12}FO_{23}$ were an independent phase, it could be considered as the member $n = 13$ of the M_nX_{2n-2} series.

$WZr_{12}FO_{23}$ units seem, as shown upon comparing Figs. 6c and 7, more regular and symmetrical than the homologous units of UY_6O_{12}. That could be a consequence of the greater dilution of the anion-deficient clusters in our phase, but also of the statistical refinement of the O(3) site. Indeed, as already shown, four different orientations of the WFO_5 octahedra are possible, obviously related to various local distributions of the $Zr(2)O_7$ and $Zr(2)O_8$ polyhedra. The statistical superposition of all these orientations agrees with the $Fm\bar{3}m$ space group but, as in many anion-deficient fluorite phases, the local symmetry of the $WZr_{12}FO_{23}$ units is likely lower (rhombohedral?). Then, the structure description in the $Fm\bar{3}m$ space group tends to minimize the local anionic and cationic relaxations, which only appear as components of the thermal vibration factors.

IV. Long-Range Ordering of the $Th_8Zr_6F_3O_{30}$ and $WZr_{12}FO_{23}$ Structural Units

The structure of $WTh_8Zr_{18}F_4O_{53}$ is built by a three-dimensional association of the $Th_8Zr_6F_3O_{30}$ and $WZr_{12}FO_{23}$ units, alternating along the three main axes of the fluorite superstructure. The fcc cationic network of the fluorite structure is preserved. Figure 8 illustrates the striking complementarity of the association of both structural units, the anion-excess one being slightly expanded and the anion-deficient one slightly contracted in comparison to the ideal fluorite structure. That gives an undulating character to the anionic planes about these units and a great stability to this structure which does not become disordered, even at 1200°C.

The association in the same proportion of anion-excess fluorite blocks of composition $MX_{2.357}$ and of anion-deficient fluorite blocks $MX_{1.846}$ forms the fluorite phase with the lowest excess of anions ever accommodated in an ordered way: $MX_{2.11}$.

The specific role of the F(1) site must be emphasized; indeed, each F(1) anion is only bonded to four Th^{4+} cations and directly connects four anion-excess blocks. As

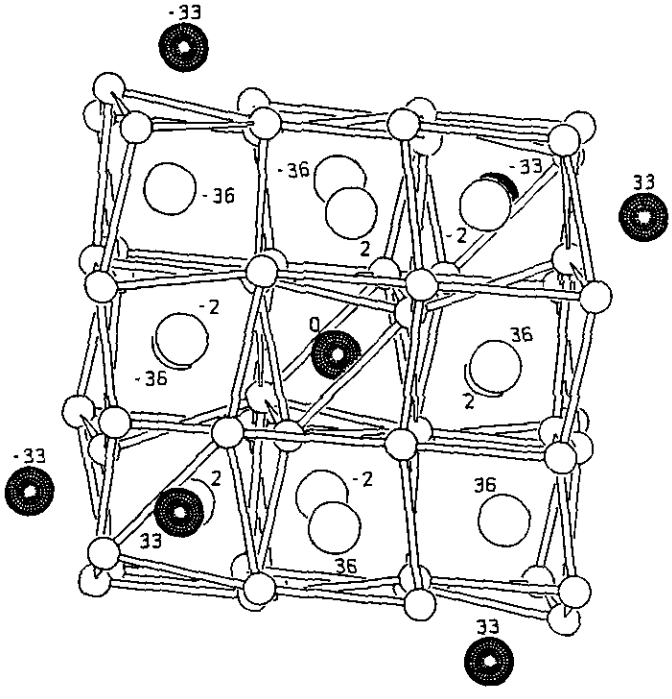

FIG. 7. Association of 12 YO_7 polyhedra about 1 UO_6 octahedron in UY_6O_{12} (Pr_7O_{12} type), to be compared to the $WZr_{12}FO_{23}$ structural unit (Fig. 6c). The neighboring U cations are also represented (U, dark spheres).

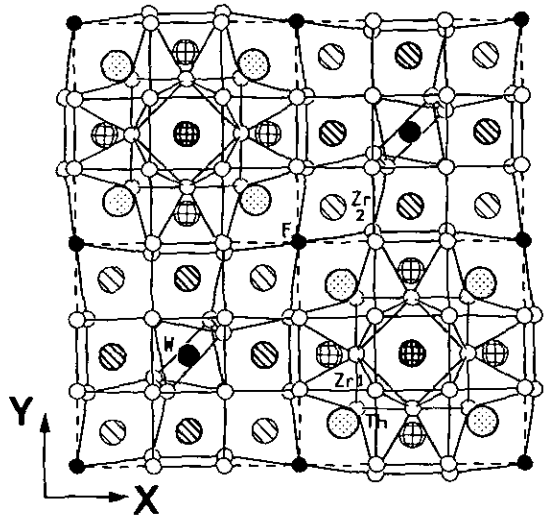

FIG. 8. Projection of the structure of $WTh_8Zr_{18}F_4O_{53}$ onto the xy plane. Only represented are the cations within the limits $-0.18 \leq z \leq 0.18$ and the anions of their coordination polyhedra. The complementary association of both kinds of clusters clearly appears. The atom symbols are almost the same as in previous figures. O–F bonds, broken lines; O–O bonds, continuous lines; darker cations, $z = 0.16$–0.18; lighter cations, $z = 0$.

previously discussed, in these last structural units, Th^{4+} cations are face-shared to ZrO_8 square antiprisms with a very short Th–Zr distance (348.2 pm), which implies a distortion of the cationic fcc network, easily observed in Fig. 8. Consequently, the Th–Th distance is lengthened to 426.1 pm between two clusters, and the electrostatic valence of the anion connecting four anion-excess units, through a common $F(1)Th_4$ tetrahedron with a long Th–F(1) bond of 260.9 pm, is rather low. Therefore, a low-charge anion like F^- is well suited to ensure the long-range stability of the association of these structural blocks. This situation is exactly the opposite of phases like $PbZr_6F_{22}O_2$ (13) or $BaTh_6F_{24}O$ (14), in which the connection between adjacent edge-shared cuboctahedral clusters needs the presence of a small number of O^{2-} anions which play an essential role in the stability of the structure.

CONCLUSION

The structure $WTh_8Zr_{18}F_4O_{53}$ is the first fluorite structure containing together anion-deficient (as, e.g., in "stabilized" zirconia or lanthanoïde oxides) and anion-excess (as, e.g., in β-U_4O_9) fragments, associated in a complementary ordered way.

Therefore, it corresponds to a conceptual advance in the field of nonstoichiometry studies and opens the way to the synthesis of new fluorite-related phases with a wide variety of cations. Indeed, the presence of cationic sites with 6-, 7-, 8-, and 10-fold coordination and the possibility to correlate the cationic charge and O/F substitutions on various sites give a great potential adaptability to this new structure type. In a further work, some of the phases prepared via such substitutions will be presented.

ACKNOWLEDGMENTS

The authors thank Professor J. Strähle and Dr. W. Hiller from Tübingen University for crystal recording, and Professor D. J. M. Bevan for his judicious suggestions.

REFERENCES

1. R. B. Von Dreele, L. Eyring, A. L. Bowman, and J. L. Yarnell, *Acta Crystallogr. B* **31,** 971 (1975).
2. S. F. Bartram, *Inorg. Chem.* **5,** 749 (1966).
3. M. R. Thornber, D. J. M. Bevan, and J. Graham, *Acta Crystallogr. B* **24,** 1183 (1968).
4. J. Zhang, R. B. Von Dreele, and L. Eyring, *J. Solid State Chem.* **104,** 21 (1993).
5. E. Schweda, *in* "Key Engineering Materials," Vol. 68, p. 187. Trans Tech Publications, 1992.
6. D. J. M. Bevan, I. E. Grey, and B. T. M. Willis, *J. Solid State Chem.* **61,** 1 (1986).
7. J. W. Pierce and H. Y. P. Hong, *in* "Proceedings, 10th Rare Earth Conference, Carefree, Arizona, 1973, Vol. A2, p. 52.
8. D. J. M. Bevan, O. Greis, and J. Strähle, *J. Solid State Chem.* **44,** 75 (1982).
9. B. Frit and J. P. Laval, *J. Solid State Chem.* **39,** 85 (1981).
10. G. M. Sheldrick, "SHELXTL, a Siemens Package for Crystal Structure Determination," 1990.
11. J. H. Burns, R. D. Ellison, and H. A. Levy, *Acta Crystallogr. B* **24,** 230 (1968).
12. A. Mikou, J. P. Laval, B. Frit, and J. Senegas, *Rev. Chim. Miner.* **22,** 115 (1985).
13. J. P. Laval and B. Frit, *Rev. Chim. Miner.* **20,** 368 (1983).
14. A. Mikou, J. P. Laval, and B. Frit, *Rev. Chim. Miner.* **24,** 315 (1987).
15. I. D. Brown, *in* "Structure and Bonding in Crystals" (M. O'Keeffe and A. Navrotsky, Eds.). Academic Press, New York, 1981.
16. D. J. M. Bevan, O. Greis, and J. Strähle, *Acta Crystallogr. A* 36, 889 (1980).
17. B. Frit, G. Roult, and J. Galy, *J. Solid State Chem.* **48,** 246 (1983).